Strain Transfer of Bonded FBG Sensor for Coal Mining Similar Model

Guihua Zhang

School of College, Xi'an University of Science and Technology, Xi'an 710054, China

zhangguihua@xust.edu.cn

***Abstract*-To accurately monitor the strain of a host with low strength, a new strain transfer model is proposed for the substrate FBG sensor. In the strain transfer model, the mechanical properties of the host are taken into consideration. The strain relationship between the fiber core and the host is obtained. The theoretical approach was verified by numerical simulation and experimental results. The influences of the mechanical parameters of the host on the strain transfer are analyzed. It is concluded that the strain transfer rate increases nonlinearly with the increase of the shear modulus of the host. The shear modulus of the host has different influence in different strain ranges; for the low strength host, the mechanical parameters of the host have great influence on the strain transfer rate. These results provide theoretical guidelines for the FBG sensor applications in low strength host.**

Keywords- Fiber Bragg Grating; Strain Transfer; Similar Model; Mechanical Parameter

I. INTRODUCTION

As the main test method of rock mechanics, coal mining similar models have great potential to analyze the formation stress in underground mining engineering [1]. In the mining similar model, we can evaluate the movement of overburdened strata by monitoring the internal strain [2]. The fiber Bragg grating sensor (FBGs) method was adopted to monitor internal strain, and has been tested for feasibility in coal mining models [3-5]. The new method of FBGs based on similar material was developed to monitor strain in tunnel excavation [6]. However, research on FEG-based mine models is still limited. It is necessary to study the strain transfer of the substrate FBG sensor for coal mining in a similar model.

There are two popular types of FBGs available: cylindrical embedded FBGs and substrate FBGs. The strain transfer of cylindrical embedded FBGs has been studied by many researchers [7-9]. It was assumed that there is identical strain in the fiber core and the host [10]; however, there are different strains in the fiber core and the host [11]. This is because the adhesive layer and the coating layer can consume energy. Similarly, the same strain rate has been considered between the FBGs center and the host [12]. However, there is still limited research on strain transfer for the substrate FBG sensor. A main reason for this is the asymmetry of the substrate FBG sensor, which increases the difficulty of analysis. A strain transfer model of a substrate fiber sensor was established to evaluate the interaction between the host material and the fiber core [13-15]. The finite element method (FEM) was used to simulate the influence of the geometric parameters of the adhesive layer of the substrate FBG sensors [16]. However, in those analyses, it was assumed that the mechanical properties of the host did not influence strain transfer. Monette found that the strain transfer of FBG was related to the elasticity modulus of the host [17], but they did not provide the definite relationship between the strain transfer and the elasticity modulus of the host. Therefore, we must consider the mechanical characteristics of the host in order to improve the substrate FBG strain transfer model to predict strain in coal mining models.

This study proposes an improved strain transfer model of the substrate FBG which is suitable for a coal mining model. From the proposed model, a theoretical formula is derived and used to predict the strain transfer relationship between the coal mining model and the fiber core in consideration of the mechanical properties of the host. Then, a numerical simulation by FEM and practical experiments are conducted to validate the theoretical predictions.

II. THEORETICAL METHODS

A model of the substrate FBG sensor for a coal model is shown in Fig. 1. The strain transfer between the fiber core and the host is derived based on the following assumptions:

1) Materials of all layers of the sensor are isotropic and elastic.

2) Only the coal model is subjected to the uniform axial stress.

3) All the interfaces are perfectly aligned, and displacement exists only in the axial direction.

4) The middle layers can also react to the model, thereby reducing the model's strain. The depth of influence of middle layer on the model is hh=1mm.

DOI: 10.5963/JBAP0403001

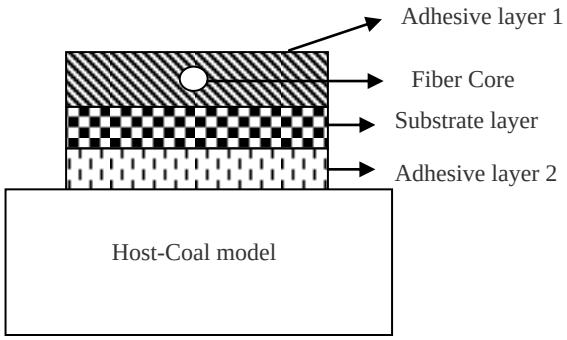

(a) Cross-section

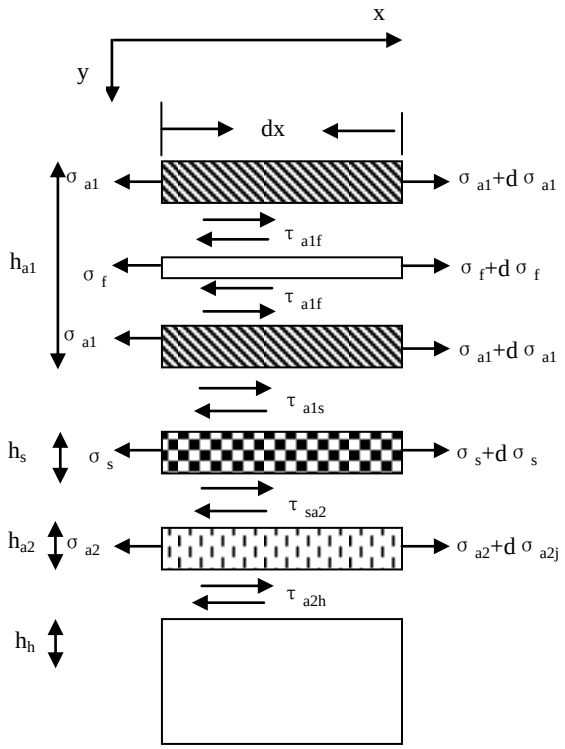

(b) Stress distribution of the longitudinal section of the substrate FBG sensor

Fig. 1 Model of the substrate FBG sensor for coal model

In Fig. 1, σ, τ and u represent the axial stress, shear stress and displacement, respectively; h denotes the thickness; E and G represent Young's modulus and the shear modulus, respectively; subscripts a1, f, s, a2 and h represent adhesive layer 1, FBG layer, substrate layer and adhesive layer 2, respectively; r_f represents the radius of the fiber core; b is the thickness of the sensor; 2L is the length of the sensor; τ_{a1f}, τ_{a1s}, τ_{sa2}, τ_{a2h} are the shear stress between the adhesive layer 1 and FBG layer, the adhesive layer 1 and the substrate layer, the substrate layer and adhesive layer 2, and the substrate layer and the host structure, respectively.

Under the above assumptions, the force equilibrium equation for adhesive layer 1 is expressed as follows:

$$d\sigma_{a1}(bh_{a1}-\pi r_f^2)+\tau_{a1f}2\pi r_f dx+\tau_{a1s}bdx=0 \tag{1}$$

where

$$\frac{d\sigma_{a1}}{dx}=\frac{-\tau_{a1s}b-\tau_{a1f}2\pi r_f}{bh_{a1}-\pi r_f^2} \tag{2}$$

Similarly, the force equilibrium equation for the FBG layer, substrate layer and adhesive layer 2 are expressed as follows:

DOI: 10.5963/JBAP0403001

$$\frac{d\sigma_f}{dx}=\frac{2}{r_f}\tau_{a1f} \tag{3}$$

$$\frac{d\sigma_s}{dx}=\frac{\tau_{a1s}-\tau_{sa2}}{h_s} \tag{4}$$

$$\frac{d\sigma_{a2}}{dx}=\frac{\tau_{sa2}-\tau_{a2h}}{h_{a2}} \tag{5}$$

It is assumed that there are identical strain gradients in all layers:

$$\frac{d\varepsilon_f}{dx}=\frac{d\varepsilon_{a1}}{dx}=\frac{d\varepsilon_s}{dx}=\frac{d\varepsilon_{a2}}{dx} \tag{6}$$

Because E_s is greater than E_{a1} and E_{a1}, equations (2)-(6) obtain:

$$\tau_{a2h}=-E_s(h_s+\frac{E_f}{E_s}\frac{\pi r_f^2}{b})\frac{d\varepsilon_f}{dx} \tag{7}$$

$$\tau_{sa2}=-E_s(h_s+\frac{E_f}{E_s}\frac{\pi r_f^2}{b})\frac{d\varepsilon_f}{dx}=\tau_{a2h} \tag{8}$$

$$\tau_{a1s}=E_f\frac{\pi r_f^2}{b}\frac{d\varepsilon_f}{dx} \tag{9}$$

$$\tau_{a1f}=\frac{E_f r_f}{2}\frac{d\varepsilon_f}{dx} \tag{10}$$

It is assumed that the shear stress of every layer is linear by its depth; shear stress expressions are τ_{a1}, τ_s, τ_{a2}.

$$\tau_{a1}=\frac{\tau_{a1s}-\tau_{a1f}}{\frac{h_{a1}}{2}-r_f}y+\frac{\tau_{a1s}(-r_f-\frac{h_{a1}}{2})+\tau_{a1f}h_{a1}}{\frac{h_{a1}}{2}-r_f} \tag{11}$$

where $\frac{h_{a1}}{2}+r_f\le y\le h_{a1}$.

$$\tau_s=\frac{\tau_{sa2}-\tau_{a1s}}{h_s}(y-h_{a1})+\tau_{a1s} \tag{12}$$

where $h_{a1}\le y\le h_{a1}+h_s$.

$$\tau_{a2}=\frac{\tau_{a2h}-\tau_{sa2}}{h_{a2}}(y-h_{a1}-h_s)+\tau_{sa2} \tag{13}$$

where $h_{a1}+h_s\le y\le h_{a1}+h_s+h_{a2}$.

For the coal model, τ_h is linear with the depth of the host. When $y=h_n+h_c+h_j+h_m$, $\tau_m=0$; when $y=h_n+h_c+h_j$, $\tau_m=\tau_{mj}$.

Thus, we obtain:

DOI: 10.5963/JBAP0403001

$$\tau_h = \frac{\tau_{a2h}}{h_h}(h_{a1} + h_s + h_{a2} + h_h - y) \tag{14}$$

where $h_{a1}+h_s + h_{a2} \le y \le h_{a1} + h_s + h_{a2} + h_h$.

Substituting formula (14) into $\tau_h = G_h \frac{du}{dy}$ and integrating with respect to y, we obtain:

$$\begin{aligned} \int_{h_{a1}+h_s+h_{a2}}^{h_{a1}+h_s+h_{a2}+h_h} G_h \frac{du}{dy} dy &= G_h(u_h - u_{a2}) = -\frac{1}{2} h_h (E_s h_s + E_f \frac{\pi r_f^2}{b}) \frac{d\varepsilon_f}{dx} \\ &= \int_{h_{a1}+h_s+h_{a2}}^{h_{a1}+h_s+h_{a2}+h_h} \frac{\tau_{a2h}}{h_h}(h_{a1} + h_s + h_{a2} + h_h - y) dy \end{aligned} \tag{15}$$

Differentiating formula (15) with respect to x, we obtain:

$$\varepsilon_{a2} = \varepsilon_h + \frac{1}{2} h_h (E_s h_s + E_f \frac{\pi r_f^2}{b}) \frac{d^2\varepsilon_f}{dx^2} \tag{16}$$

Similarly, the strain transfer equation for the substrate layer, adhesive layer 2 and FBG are ε_s, ε_{a1}, ε_f, respectively.

$$\varepsilon_s = \varepsilon_{a2} + \frac{E_s h_{a2}}{G_{a2}}(h_s + \frac{E_f}{E_s}\frac{\pi r_f^2}{b}) \frac{d^2\varepsilon_f}{dx^2} \tag{17}$$

$$\varepsilon_{a1} = \varepsilon_s + \frac{E_s}{2G_s} h_s^2 \frac{d^2\varepsilon_f}{dx^2} \tag{18}$$

$$\varepsilon_f = \varepsilon_s + \frac{E_s}{2G_s} h_c^2 \frac{d^2\varepsilon_f}{dx^2} - \frac{E_f}{G_{a1}}(\frac{\pi r_f^2}{b} + \frac{r_f}{2})(\frac{h_{a1}}{4} - \frac{r_f}{2}) \frac{d^2\varepsilon_f}{dx^2} \tag{19}$$

According to equations (16)-(19), we obtain:

$$\frac{d^2\varepsilon_g(x)}{dx^2} - k^2 \varepsilon_g(x) = -k^2 \varepsilon_h(x) \tag{20}$$

Where

$$\frac{1}{k^2} = \frac{E_s h_{a2}}{G_{a2}}(h_s + \frac{E_f}{E_s}\frac{\pi r_f^2}{b}) + \frac{E_s}{2G_s} h_s^2 - \frac{E_f}{G_{a1}}(\frac{\pi r_f^2}{b} + \frac{r_f}{2})(\frac{h_{a1}}{4} - \frac{r_f}{2}) + \frac{1}{2} h_h \frac{(E_s h_s + E_f \frac{\pi r_f^2}{b})}{G_h}$$

The general solution of formula (20) is as follows:

$$\varepsilon_f(x) = C_1 e^{kx} + C_2 e^{-kx} + \varepsilon_h(x) \tag{21}$$

where C_1 and C_2 are the integration constants determined by boundary conditions.

The boundary conditions are given as $\varepsilon_f(L) = \varepsilon_f(-L) = 0$.

Thus, C_1 and C_2 can be expressed as:

$$C_1 = C_2 = -\frac{\varepsilon_h}{2\cosh(kL)} \tag{22}$$

Substituting equation (22) into equation (21), we obtain:

$$\varepsilon_f(x) = \varepsilon_h(x)\left[1 - \frac{\cosh(kx)}{\cosh(kL)}\right] \tag{23}$$

DOI: 10.5963/JBAP0403001

Along the fiber length, the strain transfer rate is expressed as:

$$\alpha = \frac{\varepsilon_f(x)}{\varepsilon_h(x)} = 1 - \frac{\cosh(kx)}{\cosh(kL)} \tag{24}$$

The average strain transfer rate is expressed as:

$$\bar{\alpha} = \frac{\varepsilon_f(x)}{\varepsilon_h(x)} = \frac{2\int_0^L \left[1 - \frac{\cosh(kx)}{\cosh(kL)}\right] dx}{2L} = 1 - \frac{\sinh(kL)}{kL\cosh(kL)} \tag{25}$$

From equation (25), we can obtain the average strain transfer rate related to the mechanical parameters of the host and the substrate layer.

III. NUMERICAL VALIDATION AND PARAMETER ANALYSIS

A. Numerical Validation

Numerical analysis was conducted to validate the theoretical predictions with ANASYS software. Due to the geometry, only half of the substrate FBGs is analyzed. Fig. 2 shows the finite element model. All parameters are listed in Table 1.

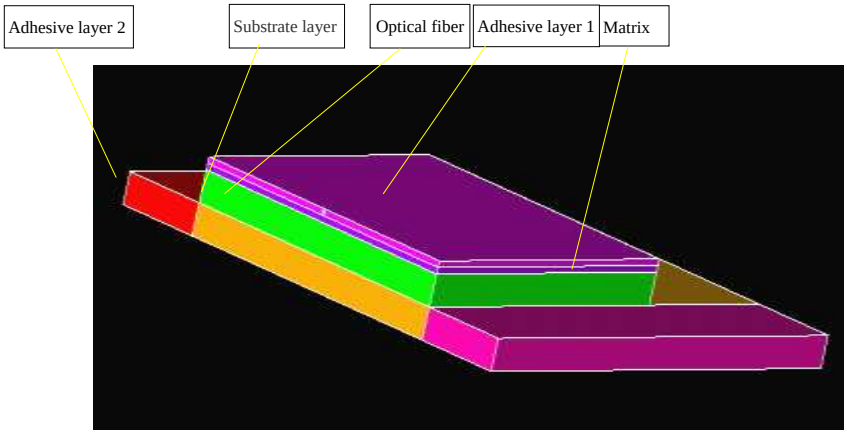

Fig. 2 Finite element model

TABLE 1 ASSIGNED PARAMETERS OF THE FBG MODEL

Parameter	Value
Radius of fiber core, r_f (μm)	62.5
Young's modulus of fiber core, E_f (GPa)	72
Poisson's ratio of fiber core, γ_g	0.17
Young's modulus of adhesive layer 1, E_{a1}(MPa)	25
Shear modulus of adhesive layer 1, G_{a1}(MPa)	10
Thickness of adhesive layer 1 h_{a1}(mm)	0.2
Young's modulus of substrate, E_s(MPa)	10^5
Shear modulus of substrate, G_s(GPa)	40
Thickness of substrate, h_s(*mm*)	0.2
Young's modulus of adhesive layer 2, E_{a2}(MPa)	25
Shear modulus of adhesive layer 2, G_{a2}(MPa)	10
Young's modulus of coal model, E_h(MPa)	227
Shear modulus of coal model, G_h(MPa)	97

DOI: 10.5963/JBAP0403001

Thickness of adhesive layer 2 $h_{a2}(mm)$	0.2
Length of FBG sensor, $2L(cm)$	4

The sensor and the host are modeled with solid 185, and all model elements demonstrate linear elastic behavior. An axial load of 16N is applied to the host. Fig. 3 shows the axial strain nephogram of the fiber core by ANASYS.

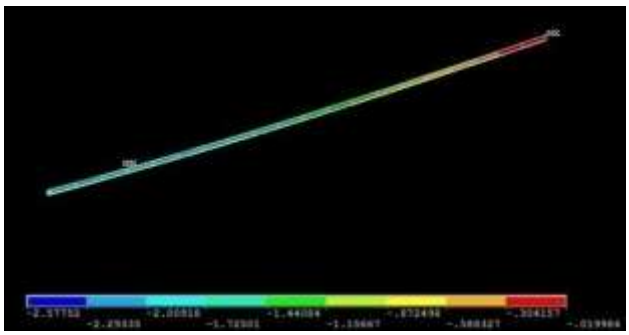

Fig. 3 Axial strain nephogram of the fiber core by the ANASYS

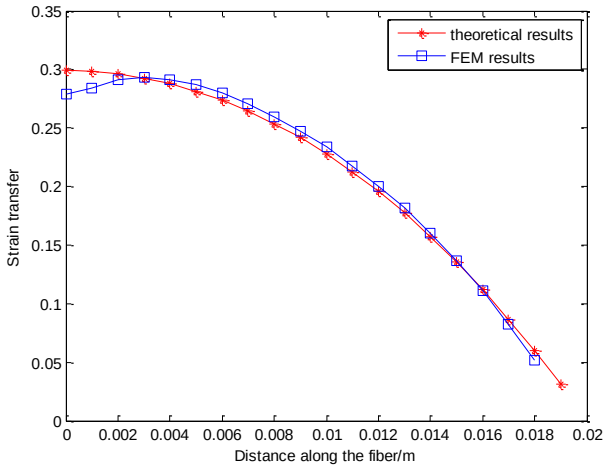

Fig. 4 Strain transfer rate comparison of theoretical analysis and ANASYS results

In Fig. 4, the strain transfer rates by ANASYS are compared with that obtained by equation (24). As can be seen in Fig. 4, the two curves are nearly identical, and theoretical results agree with ANASYS results. The average strain transfer rate $\bar{\alpha}_{ANASYS}$ is 0.2000 as calculated by ANASYS. The values in Table 1 are substituted into equation (25) to obtain the theoretical result $\bar{\alpha}_{\text{theoretics}} = 0.2019$. There is 0.9% strain relative error between the theoretical result and the ANASYS result. It is further shown that the theoretical predictions are in good agreement with the ANASYS results.

B. Parametric Analysis

Based on theoretical analysis, the influence rates of parameters on the strain transfer rate are discussed. The parameters represent the mechanical properties of the substrate layer and the host layer. The parameters of the fiber core and adhesive layer are listed in Table 1, and will be used in the following subsections to simulate the effects of G_h and E_s on the average strain transfer rates.

Fig. 5 shows the average strain transfer rate as a function of the shear modulus of the host layer. As can be seen, the strain transfer rate increases with an increasing host shear modulus, and this tendency becomes more rapid with smaller shear modulus values. When the shear modulus changes in the range of 10 to 500 MPa, the slope of the curve varies greatly and the host shear modulus has great influence on the strain transfer rate. When the shear modulus of the host is more 500 MPa, the curve is smoother and the host shear modulus has little influence on the strain transfer rate. Results indicate that when the value of the host shear modulus is small, the host shear modulus must be considered as an important parameter in the application of FBG sensors.

As shown in Fig. 5, the average strain transfer rate decreases with an increase in the elastic modulus of the substrate layer.

DOI: 10.5963/JBAP0403001

This is a consequence of the fact that the small host elastic modulus augments the efficiency of load transfer from the host material to the fiber core. For the coal mining model, the low strength material necessitates that we consider the influence of the mechanical parameters of the host on the strain transfer.

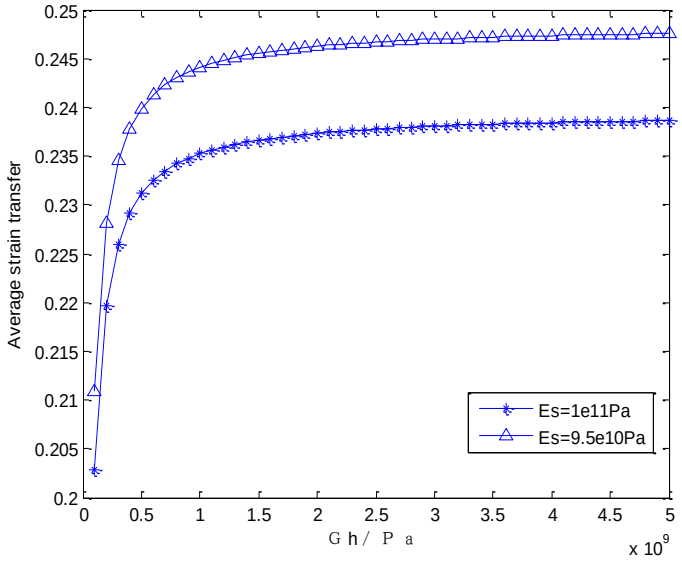

Fig. 5 Average strain transfer rate in the shear modulus of the host

IV. EXPERIMENT VALIDATION

Laboratory tests are performed using FBG sensors to verify our theoretical analysis. The experimental model is shown in Fig. 6.

Fig. 6 Experiment model

Three substrate FBG sensors, FBG1, FBG2 and FBG3, were embedded in the strata of the coal mine model to obtain the strain of the coal model. For comparison, three dial indicators were placed near the corresponding FBG sensors to obtain the displacements of the strata. The three dial indicators are DI1, DI2 and DI3.

Fig. 7 shows that the wavelength shifts of FBG2 and the displacements of DI2 vary with the mining distance. It can be seen that the displacements vary linearly with the wavelength shifts, with a linear correlation coefficient R is 0.92, allowing comparison of results between the FBGs and dial indicators.

DOI: 10.5963/JBAP0403001

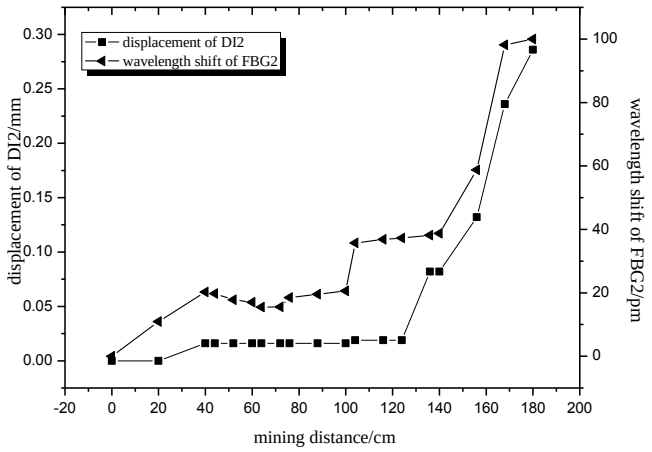

Fig. 7 Wavelength shifts of FBG2 and displacements of DI2 varying with mining distance

The host strain is the ratio of the displacement recorded by the dial indicator to the depth of corresponding strata. The experimental average strain transfer rate is the ration of the fiber strain by the FBG sensor to the host strain.

In the experiments, the strain transfer rates of FBG1, FBG2 and FBG3 were 0.17, 0.17 and 0.13, respectively. The average strain transfer coefficient of three sensors $\overline{\alpha}_{experiment}$ was 0.16. There was a 20% strain relative error between experimental result and with the theoretical result, while the error was 0.9% between the theoretical and FEM results.

The values in Table 1 are substituted into the strain transfer formula by Zhou [9] where they neglect the influence of the mechanics parameter of the host. The average strain transfer rate was 0.28, with a 75% between theoretical result by Zhou [9] and the experimental result. Therefore, there is a great difference in strain transfer rate when the mechanical parameter of the host is or is not taken into consideration. The result in our theoretical model is closer to the experiment result, thus the mechanical parameter of the host cannot be neglected for the coal mining model.

Summarily, our theoretical prediction is in agreement with the ANASYS results. The theoretical model can predict the actual strain of the coal mining model. Therefore, based on the theoretical model, the FBG can be used to accurately measure the strain in the coal model.

V. CONCLUSION

FBGs has great potential for analysis of the internal strain of the coal mining model. This paper proposed a strain transfer model for a coal mining similar model by introducing the mechanical properties of the host to theoretically predict the strain transfer relationship between the fiber core and the coal mine model. Finally, we arrived at the following conclusions:

(1) In the consideration of the mechanics parameter of the host, the strain transfer rate between the fiber core and the host is theoretically obtained.

(2) The theoretical results are validated by ANASYS and experiments. There is 0.9% strain relative error between the theoretical result and the ANASYS result.

(3) The shear modulus of the host has different influences in different strain ranges. When the shear modulus of the host is less than 500MPa, it has great influence on the strain transfer rate. When the shear modulus of the host is more than 500MPa, it has little influence on the strain transfer rate.

(4) For the low strength host, we must consider the influence of the mechanical parameters of the host on the strain transfer. For the high strength host, we can neglect the influence of the mechanical parameters of the host.

ACKNOWLEDGMENTS

This work was supported by National Natural Science Foundation of China (51174280). Authors are grateful for the support.

REFERENCES

[1] Zuo Bao-cheng, Chen Cong-xin, Liu Cai-hua, et al., "Research on similar material of simulation experiment," *Rock and Mechanics*, vol. 25, no. 11, pp. 1805-1808, 2004.

DOI: 10.5963/JBAP0403001

[2] Qiao Lan, Ouyang Zhenhua, Lai Xingping, et al., "In-situ stress measuring and its result analysis in sanshandao gold mine of China," *Journal of University of Science and Technology Beijing*, vol. 26, no. 6, pp. 569-571, 2004.

[3] Yong Zhao, Zhongqiang Li, and Yue Dong, "Design and experiments on a wide range fiber Bragg grating sensor for health monitoring of coal mines," *International Journal for Light and Electron Optics*, vol. 125, no. 20, pp. 6287-6290, 2014.

[4] JoAnn R. Gage, Herbert F. Wang, Dante Fratta, et al., "In situ measurements of rock mass deformability using fiber Bragg grating strain gauges," *International Journal of Rock Mechanics and Mining Sciences*, vol. 71, no. 10, pp. 350-361, 2014.

[5] Chai Jing, Zhao Wen-hua, Li Yi, et al., "FBG monitoring test on settlement deformation of overlaying strata in similar models," *Journal of China coal Society*, vol. 38, no. 1, pp. 55-60, 2013.

[6] Wang et al., "Trifarious FBG sensor strain transfer characteristics and its applications to tunnel excavation model test," *Journal of Engineering Geology*, vol. 21, no. 2, pp. 182-189, 2013, [doi:10.3969/j.issn.1004-9665.2013.02.002].

[7] Ru jun Wu, Bailin Zheng, Zhigang Liu, Pengfei He, and Yuegang Tan, "Analysis on strain transfer of a pasted FBG strain sensor," *International Journal for Light and Electron Optics*, vol. 125, no. 17, pp. 4924-4928, 2014.

[8] Li Dongsheng and Zhou zhi, "Strain transferring analysis of embedded fiber Bragg grating sensors," *Chinese Journal of Theoretical and Applied Mechnics*, vol. 37, no. 4, pp. 435-441, 2005.

[9] Zhou Zhi, Li Ji-long, and Ou Jin-ping, "Interface strain transfer mechanism and error modification of embedded FBG strain sensors," *Journal of Harbin Institute of Technology*, vol. 38, no. 1, pp. 49-54, 2006.

[10] Farhad Ansari and Yuan Libo, "Mechanics of bond and interface shear transfer in optical fiber sensors," *Journal of Engineering Mechanics*, vol. 124, no. 4, pp. 385-394, 1998.

[11] C. C. Cheng, Y. L. Lo, and W. Y. Li, "Accurate simulations of reflective wavelength spectrum of surface-bonded fiber Bragg grating," *Applied Optics*, vol. 49, no. 17, pp. 3394-3402, 2010 [doi:10.1364/AO.49.003394].

[12] Li Dong-sheng and Li Hong-nan, "Strain transferring analysis of embedded fiber Bragg Grating sensors," *Chinese Journal of Theoretical and Applied Mechanics*, vol. 37, no. 4, pp. 435-441, 2005.

[13] S. C. Her and C. Y. Huang, "Effect of coating on strain transfer of optical fiber Bragg sensors," *Sensors*, vol. 11, no. 7, pp. 6926-6941, 2011 [doi:10.3390/s110706926].

[14] Zhao Hai-tao, Wang Quan-bao, Qiu Ye, et al., "Strain transfer of surface-bonded fiber Bragg grating sensors for airship envelope structural health monitoring," *Journal of Zhejiang University-Science A*, vol. 13, no. 7, no. 539-545, 2012.

[15] Sun Li, Yue Chuan-yun, and Song Yan-sheng, "Strain transfer analysis of substrate fiber Bragg grating sensor," *Journal of Optoelectronics Laser*, vol. 24, no. 5, pp. 849-853, 2013.

[16] K. T. Wan, C. K. Y. Leung, and N. G. Olson, "Investigation of strain transfer for surface-attached optical fiber strain sensors," S*mart Materials and Structures*, vol. 17, no. 3, p. 035037, 2008 [doi:10.1088/0964-1726/17/3/035037].

[17] L. Monette, M. P. Anderson, S Ling, et al., "Effect of modulus and cohesive energy on critical fibre length in fibre-reinforce composites," *Journal of Material Science*, no. 27, pp. 4393-4405, 1992.

DOI: 10.5963/JBAP0403001